WARWICK
THE UNIVERSITY OF WARWICK

Manuscript version: Author's Accepted Manuscript
The version presented in WRAP is the author's accepted manuscript and may differ from the published version or Version of Record.

Persistent WRAP URL:
http://wrap.warwick.ac.uk/163303

How to cite:
Please refer to published version for the most recent bibliographic citation information. If a published version is known of, the repository item page linked to above, will contain details on accessing it.

Copyright and reuse:
The Warwick Research Archive Portal (WRAP) makes this work by researchers of the University of Warwick available open access under the following conditions.

© 2022 Elsevier. Licensed under the Creative Commons Attribution-NonCommercial-NoDerivatives 4.0 International http://creativecommons.org/licenses/by-nc-nd/4.0/.

Publisher's statement:
Please refer to the repository item page, publisher's statement section, for further information.

For more information, please contact the WRAP Team at: wrap@warwick.ac.uk.

warwick.ac.uk/lib-publications

For submission to Special Issue "Celebrating Fifty Years of the Journal of Inorganic Biochemistry"

A metallothionein from an open ocean cyanobacterium removes zinc from the sensor protein controlling its transcription

Alevtina Mikhaylina,[1,2] Luke Scott,[1] David J. Scanlan[2] and Claudia A. Blindauer[1,*]

[1] Department of Chemistry, University of Warwick, UK
[2] School of Life Sciences, University of Warwick, UK

Email: c.blindauer@warwick.ac.uk

Abstract

Bacterial metallothioneins are known for a limited range of phyla including cyanobacteria. We have characterised the BmtA from the marine cyanobacterium *Synechococcus* sp. WH8102 (SynBmtA). This strain inhabits the open ocean, one of the most nutrient-poor environments on Earth, with very low total and free Zn^{2+} concentrations. Therefore, the presence of a metallothionein, usually associated with zinc and cadmium tolerance, in this strain is intriguing. Previous transcriptomics work revealed that unprecedentedly, expression of SynBmtA is activated by the "zinc uptake regulator" SynZur at elevated [Zn^{2+}]. SynBmtA binds four Zn^{2+} ions, and its first 37 residues adopt the zinc-finger fold characteristic of BmtAs. In contrast, sequence similarity to other BmtAs in the C-terminal stretch is low. This is expected to impact especially on the most reactive site in zinc-transfer reactions. Indeed, chelators were unable to extract Zn^{2+} from SynBmtA, even in the presence of denaturant. This indicates an extremely stable protein fold, with no accessibility to any bound zinc ions in the folded protein. In addition, the zinc-binding affinity of SynBmtA exceeds those of any other metallothioneins. Apo-SynBmtA is capable of removing zinc from the sensory site of SynZur, providing one possible avenue of de-activating transcription of the *synbmtA* gene. All of these properties are consistent with a role in safely sequestering any excess zinc, to prevent toxic effects. The fact that this strain stores zinc in a metallothionein rather than employing an efflux pump implies that zinc is a valuable resource for *Synechococcus* sp. WH8102 and related strains.

Keywords: Zinc, cyanobacteria, metallothionein, zinc uptake regulator, ESI-MS

1. Introduction

Metallothioneins (MTs) have been a staple topic in Inorganic Biochemistry throughout the decades of JIB's existence, and indeed, there have been so far several hundred manuscripts in JIB dealing with these intriguing small metal-binding proteins. Since their discovery in horse kidney in 1957 by Margoshes and Vallee [1], they have been found in the majority of known organisms [2]. Although they are all defined by a high proportion of cysteine residues in their sequence and are all involved in metal binding, their structures and functions are highly diverse [3], and it is likely that this superfamily is polyphyletic [4].

The present study concerns a new representative of a major family of bacterial metallothioneins. The presence of MTs in bacteria was first indicated in a cyanobacterium [5] and some years later in *Pseudomonas putida* [6]. Although a range of bacterial genomes have been screened for genes that may encode cysteine-rich proteins [7], only two different families of confirmed MTs are known in bacteria, namely the BmtAs [8], which occur in only a few bacterial genera including cyanobacteria, pseudomonads, a few α-proteobacteria and one firmicute, and the MymTs, which are restricted to mycobacteria [9]. Two members of the BmtA family are now structurally characterised, the prototype SmtA from the freshwater cyanobacterium *Synechococcus* sp. PCC 7942 [10], and the PflQ2 MT from *Pseudomonas fluorescens* Q2-87 [11], with some data at the protein level also available for the BmtAs from *Anabaena* sp. PCC 7120, *Pseudomonas aeruginosa PAO1*, and *Pseudomonas putida* KT2440 [12].

Transcription of BmtAs in freshwater cyanobacteria, including *Synechococcus elongatus* sp. PCC 7942 [13], *Oscillatoria brevis* [14], and *Anabaena* sp. PCC 7120 [15], is induced primarily by Zn^{2+} and Cd^{2+}, with Zn^{2+} being the strongest inducer of *smtA* expression [13]. Mutants unable to synthesise SmtA are hypersensitive towards Zn^{2+} and Cd^{2+} [16]. Metal-dependent inducibility is mediated by the zinc excess sensors SmtB [13], BxmR [14] and AztR [17], respectively, which repress MT transcription in the absence of excess Zn^{2+}. From these studies, it would appear that the primary role of cyanobacterial MTs is to provide tolerance towards excess Zn^{2+}. We were therefore surprised to discover *bmtA* genes in oligotrophic *Synechococcus* strains [18-20]. These strains proliferate in the most nutrient-depleted regions of the world's oceans that typically also display zinc scarcity [21]. Even more intriguingly, in one of these strains, *Synechococcus* sp. WH8102, the promoter region of the *bmtA* gene was predicted to contain two binding sites for the "zinc uptake regulator" Zur [20] – which typically regulates responses to zinc scarcity rather than excess [22,23]. The most common mode of action of Zur sensors is the de-repression of *znuABC* uptake systems under zinc-depleted conditions [23]. Our recent work has shown that this is also the case for *Synechococcus* sp. WH8102 [24]. Most significantly though, we found that zinc-bound SynZur activates *bmtA* transcription at elevated zinc concentrations. Thus, *bmtA* transcript abundance, and by inference BmtA protein abundance, correlates with total intracellular [Zn], and thus SynBmtA still deals with excess zinc, like other MTs. The unprecedented activation of a bacterial metallothionein gene by a Zur sensor not only enables optimal growth over a large range of external zinc concentrations, but also supports changes in cellular zinc quotas over more than two

orders of magnitude [24]. Such a degree of variation is not commonly observed in either pro- or eukaryotic cells. Even *E. coli* over-expressing SmtA only showed a 3-fold increase in zinc accumulation [25]. However, similarly large variations in zinc quotas are mirrored in field samples of *Synechococcus* in the Sargasso Sea [26], the original habitat of the WH8102 strain [27]. Favouring safe storage over efflux may suggest that zinc is a valuable resource worth banking for later utilisation.

In addition, the abundance of SynBmtA has been found to increase upon phosphorus depletion [28], and the similarity in abundance patterns between SynBmtA and a predicted alkaline phosphatase led to the suggestion that the protein might serve in supplying zinc to this enzyme. The presence of *bmtA* genes particularly in *Synechococcus* strains dominating P-depleted waters also suggests a link between zinc and phosphorus metabolism in these cyanobacteria [24]. In contrast, and although MT production has been suggested to protect against cadmium toxicity [29], no regulation by Cd^{2+} was apparent [28].

The structure and regulon of SynZur is discussed elsewhere [24], but it is clear that the activity of SynZur as a transcription factor depends on its metallation state. SynZur and the protein the production of which it regulates, SynBmtA, both bind zinc and operate in the same compartment, namely the bacterial cytosol. It was therefore of interest to explore the ternary system SynZur, SynBmtA and Zn^{2+}. We also include prerequisite information on the properties and structure of SynBmtA.

2. Materials and methods

2.1. Cloning, protein expression and purification for SynBmtA

The gene for SynBmtA (*synw0359*) was amplified by PCR from genomic DNA of *Synechococcus* sp. WH8102 and inserted into the expression vector pET24a(+) (Novagen), using primers GCGCCATATGTCTACAGCAATCAAATG (forward) and CGACGAGCTCTTACTCTCCGCACTTAC (reverse) and *Nde1* and *SacI* restriction sites. The construct was used to transform *E. coli* DH5α cells, and colonies were screened with T7 primers TAATACGACTCACTATAGGG (forward) and GCTAGTTATTGCTCAGCGGT (reverse). The plasmid AM_synw0359_pET24 was isolated (QIAprep® Spin Miniprep Kit) from colonies that contained an insert of the correct size (382 bp), and the sequence of the insert was confirmed by Sanger sequencing (Eurofins-GATC, Germany). For protein over-expression, competent *E. coli* Rosetta2(DE3)pLysS (Invitrogen) were transformed with AM_synw0359_pET24 using a standard heat-shock protocol. Kanamycin (50 μg mL^{-1}) and chloramphenicol (35 μg mL^{-1}) were used as selective antibiotics. Cells from an overnight culture were grown in Luria-Bertani (LB) medium at 30 °C until an OD_{600} of 0.5-0.8 was reached, and then induced with 0.5 mM IPTG (isopropyl β-D-1-thiogalactopyranoside). At the same time 0.5 mM (final concentration) $ZnSO_4$ was also added. Cultures were left shaking overnight at 30°C, harvested by centrifugation, and stored at -20°C. For purification, cell pellets were suspended in lysis buffer (50 mM Tris-HCl (pH 8.5), 0.1 M KCl, 1 mM $ZnSO_4$, 3 mM dithiothreitol (DTT), 0.1 mM phenylmethylsulfonyl fluoride (PMSF)) at a ratio of 5 mL buffer per 1 g wet cell pellet and sonicated. The crude cell lysate supernatant after centrifugation was subjected to fractionated

chemical precipitation with ice-cold ethanol/chloroform (100:8, v/v). Precipitates were dissolved in 20 mM NH_4HCO_3 and analysed by SDS-PAGE with silver staining (Supplementary Figure S1). Fractions containing SynBmtA were pooled and further purified by size-exclusion chromatography (ÄKTA 100 FPLC fitted with a Superdex G75 HiLoad 16/60 column, GE Healthcare), using 20 mM NH_4HCO_3 pH 7.9 as elution buffer.

The preparation of fully metallated SynZur is reported elsewhere [24].

2.2. Inductively-coupled plasma optical emission spectroscopy

ICP-OES was carried out on a PerkinElmer 5300DV ICP-OES spectrometer. 1000 ppm standards for calibration of S, Zn, Cd, Cu, Ni, and Mn (Fisher Scientific) were diluted gravimetrically to make a 50 ppm mixed-element stock solution in 0.01 M HNO_3 and then this stock was gravimetrically diluted to prepare standards of 0, 0.2, 0.4, 0.6, 1, 2 and 5 ppm in 0.01 M HNO_3. Parameters for ICP-OES measurements were: argon flow rate 13.0 L min^{-1}, auxiliary gas flow rate 0.2 L min^{-1}, nebuliser flow rate 0.8 L min^{-1} and radio-frequency power 1300 W. Each sample was measured in triplicate.

2.3. Electrospray ionisation mass spectrometry

With the exception of the data in Figure 1, which were carried out on a Bruker MaXis TOF ESI-MS spectrometer, ESI-MS data were acquired on a Bruker Compact TOF ESI-MS spectrometer. Sample concentrations were typically 5-10 μM in 20 mM NH_4HCO_3 pH 7.8-7.9. The spectrometer was operated in positive mode with the following parameters: flow rate 240 μL h^{-1}, range (500 - 4500 m/z), end plate offset 500 V, capillary 3900 V, nebulizer 0.8 Bar, drying gas 4 L min^{-1} and drying gas temperature 190°C. Spectra were recorded for 1-2 minutes after stabilisation. Data analysis was carried out with Bruker Daltonics DataAnalysis 4.3. Conversion of raw ESI-MS spectra onto a true mass scale employed a maximum entropy algorithm within the range 1-80 kDa.

2.4. NMR spectroscopic studies

For $^{1}H,^{15}N$ NMR spectroscopy, SynBmtA was expressed in $^{15}NH_4Cl$-supplemented (99%, Cambridge Isotope Laboratories) minimal medium containing kanamycin (50 μg mL^{-1}) and chloramphenicol (35 μg mL^{-1}) (Supplementary Table S1). An overnight culture in LB medium was used to inoculate 1 L of minimal medium at a ratio of 1:100. Cultures were incubated with shaking at 37°C until OD_{600} reached ~1, then 0.5 mM IPTG and 0.1 mM $ZnSO_4$ were added, and the temperature was reduced to 23°C. Cells were left shaking for 24 h, and harvested by centrifugation. The protein was purified using the same protocol as unlabelled protein. The protein eluted from the SEC column was concentrated (Amicon Ultra-15, 3 kDa molecular weight cut-off; Merck Millipore), and 10% D_2O were added for field-frequency lock. 1 L of culture was sufficient to produce an NMR sample (2 mM in 20 mM NH_4HCO_3, pH 7.8) suitable for 3D $^{1}H,^{15}N$ experiments. All NMR experiments were carried out on a Bruker Avance 700 Ultrashield spectrometer fitted with a triple resonance ($^{1}H,^{13}C,^{15}N$)

cryoprobe. Operating frequencies were 700.24 MHz for ^{1}H and 70.95 MHz for ^{15}N. The water resonance was used for chemical shift referencing [30]. 2D (^{1}H,^{15}N) heteronuclear single quantum coherence NMR spectra (HSQC) were recorded with 128 data points in F1 (^{15}N) and with 2048 data points in F2 (^{1}H), whilst the 3D TOCSY-HSQC (60 ms mixing time; DIPSI2) and NOESY-HSQC (100 ms mixing time) spectra were recorded with 2048 in F3 (^{1}H), 200 data points in F1 (^{1}H), and 34 in F2 (^{15}N). Both 3D pulse programs involved gradient pulses in the Z dimension and sensitivity enhancement. The spectral width values were 17 ppm in F1 and F3, and 34 ppm in F2 dimensions, and 4 scans were used. The data were apodised and Fourier transformed into 2048×64×512 data points in the F3×F2×F1 dimensions. Data were acquired and processed using Bruker TopSpin 3.2 software, and sequential assignment was carried out in CCPN Analysis v. 3.0.3 and Sparky v. 3.114 [31].

Random coil chemical shifts for SmtA and SynBmtA were calculated based on Poulsen's sequence-specific corrections using the webserver at https://spin.niddk.nih.gov/bax/nmrserver/Poulsen_rc_CS/ [32].

2.5. Structural modelling

Homology modelling was carried out using Modeller v. 9.19 [33], using pdb 1jjd (Zn_4SmtA from *Synechococcus* sp. PCC 7942 [10]) and 6gv7 (truncated form of the A44H mutant of *P. fluorescens* Q2-87 MT [11]) as templates. The model in Figure 2D is based on the alignment shown in Figure 2B. Zinc ions were manually inserted based on a structural alignment with pdb 1jjd. We refrained from further refinement attempts since the available information does not allow any more conclusive inferences regarding the structure of the C-terminal portion. Models based on alternative alignments were also explored, but presented no advantages over the model shown.

2.6. Determination of the pH of half-displacement

Samples of native SynBmtA (20 µM) in 20 mM NH_4HCO_3 were adjusted to a range of pH values between 8.1 and 1.9 with 0.01, 0.1 and 1 M NaOH and HCl. UV-vis spectra in the range of 200-800 nm were recorded after each pH adjustment using a Varian Cary 50 Bio UV-vis spectrophotometer, Agilent Technologies. Absorption was normalised to the total volume. The data were fitted to

$$fraction\ of\ Zn-S\ bonds = \frac{\frac{10^{-\mathrm{pH}}\,\mathrm{n}}{10^{-\mathrm{pH}\left(\frac{1}{2}\right)}\mathrm{n}}}{1+\frac{10^{-\mathrm{pH}}\,\mathrm{n}}{10^{-\mathrm{pH}(1/2)}\,\mathrm{n}}}$$

2.7 De-metallation of SynBmtA

To investigate de-metallation of native SynBmtA, samples containing 10 µM SynBmtA in 20 mM NH_4HCO_3 were incubated with (i) 1 mM EDTA; (ii) 1 mM TPEN and 0.5 mM DTT; (iii) 6 M urea, 1 mM EDTA and 0.5 mM DTT (Final concentrations). Samples were left overnight and protein was separated from inorganic and low

molecular mass components using PD-10 desalting columns (Sephadex G-25, GE Healthcare). For successful preparation of apo-SynBmtA, 2.5 mL 30 μM SynBmtA in 10 mM NH_4HCO_3 were acidified to pH 3.3 with 4 μL concentrated formic acid. A PD-10 column was equilibrated with 25 mL 10 mM NH_4HCO_3 solution at pH 3.3 (120 μL concentrated formic acid was added per 100 mL buffer). 2.5 mL acidified SynBmtA was loaded onto the PD-10 column and eluted with 2.5 mL 10 mM NH_4HCO_3 buffer, pH 3.3. After further washing, the PD-10 column was re-equilibrated with 25 mL 10 mM NH_4HCO_3 buffer (pH 7.8). 2.5 mL of the acidified Zn-free BmtA sample was loaded once more onto the column and eluted with 2.5 mL 10 mM NH_4HCO_3 buffer (pH 7.8). All desalting steps were performed inside a nitrogen-filled glove bag. All solutions were purged beforehand with either nitrogen or argon. All reaction products were analysed by ESI-MS.

2.8. Determination of zinc binding affinities by competition with Quin-2

Upon successful de-metallation, ca. 12 μM apo-SynBmtA with 0.2 mM TCEP in 20 mM NH_4HCO_3 (pH 7.8) was mixed with ca. 130 μM Quin-2 (2-[(2-Amino-5-methylphenoxy)methyl]-6-methoxy-8-aminoquinoline-N,N,N',N'-tetraacetic acid tetrapotassium salt; Sigma-Aldrich) and titrated with 710 μM $ZnSO_4$ in triplicate. Although typically used as fluorescent dye, it was more convenient to measure the free Quin-2 concentration via absorbance at 261 nm using an extinction coefficient of 37500 cm^{-1} M^{-1} [34]. Zinc concentration was determined using ICP-OES. A UV-vis spectrum was measured after each addition of $ZnSO_4$ several times until the absorbance reading was stable (up to 15 minutes per addition of Zn^{2+} aliquot). The concentration of binding sites from SynBmtA were calculated by subtraction of the concentration of total Quin-2 from the total [Zn^{2+}] concentration after completion of the titration. Data were fitted using DynaFit [35] software, and an average K_D(Zn-SynBmtA) was determined from these fits. The plots are based on Quin-2 K_D(Zn) = 3.7×10^{-12} M [34], and a simple 1:1 binding model, assuming that all four Zn binding sites on SynBmtA have similar binding affinity, as is commonly found for MTs [36].

2.9. Electrophoretic Mobility Shift Assays (EMSAs)

The sensory Zn^{2+} ion was removed from Zn_2SynZur by incubation with a 100-fold excess of EDTA, followed by buffer exchange into 20 mM NH_4HCO_3 buffer by gel filtration (Sephadex G-25; GE Healthcare PD-10). Either the Zn_1SynZur generated or untreated Zn_2SynZur were diluted to the required concentration in Tris-glycine-glycerol buffer (TGG, 0.025 M Tris, 0.187 M glycine, 5% glycerol), with 1 mM DTT added to the final sample. 10 μL aliquots of 5 ng DNA (250 bp from the promoter region of the *bmtA* gene, Supplementary Figure S2) were mixed with different amounts of Zur (0 - 1 μM), either in the presence of 50 μM EDTA or 1 μM $ZnSO_4$ in TGG buffer. Samples were left at room temperature for 30 minutes and loaded onto precast WedgeWell 10-to-20%, Tris-glycine gels (Novex). PAGE was performed in EDTA-free Tris-glycine running buffer (TG, 0.025 M Tris, 0.187 M glycine) at 100 V for ~90 minutes at 4°C.

For visualisation of DNA bands, SYBR-Green I stock in DMSO (Sigma-Aldrich, 10 mg mL^{-1}) was diluted 1:10000 in TG buffer, and gels were stained for 30 minutes in a plastic container wrapped in foil to protect them from light. Visualisation was done using a luminescent image analyser (ImageQuant LAS 4000, GE Healthcare BioSciences AB).

2.10. Zinc transfer from metallated SynZur to apo-SynBmtA

Fully metallated SynZur was mixed with apo-SynBmtA at a ratio of 4:1 (20 µM and 5 µM, respectively). The mixture was set up inside a glove bag filled with nitrogen and left for 30 minutes to equilibrate. Thereafter, the reaction mixture was filtered with a 0.22 µm pore size Minisart® syringe filter (Sartorius) and analysed by ESI-MS (see 2.3.).

3. Results

3.1. The metallothionein from Synechococcus sp. WH8102 binds four Zn^{2+} ions and adopts the typical zinc-finger fold of bacterial MTs

SynBmtA was cloned from genomic DNA of *Synechococcus* sp. WH8102 and over-expressed as full-length protein without any fusion tags. The protein was purified by chemical precipitation and size-exclusion chromatography in ammonium bicarbonate buffer at pH 7.8 (Supplementary Figure S1), which in our experience preserves the metallation state established during expression [37-40]. The molecular weight of the apo-protein was determined by Electrospray Ionisation Mass Spectrometry (ESI-MS) at pH 2 (Figure 1A). The deconvoluted neutral mass (5619.32 Da) agrees well with the theoretical neutral mass expected for full-length SynBmtA (see Figure 2B for sequence) devoid of the N-terminal methionine (5620.42 Da), which is expected to be cleaved by aminopeptidase [41], as previously observed for SmtA as well [12].

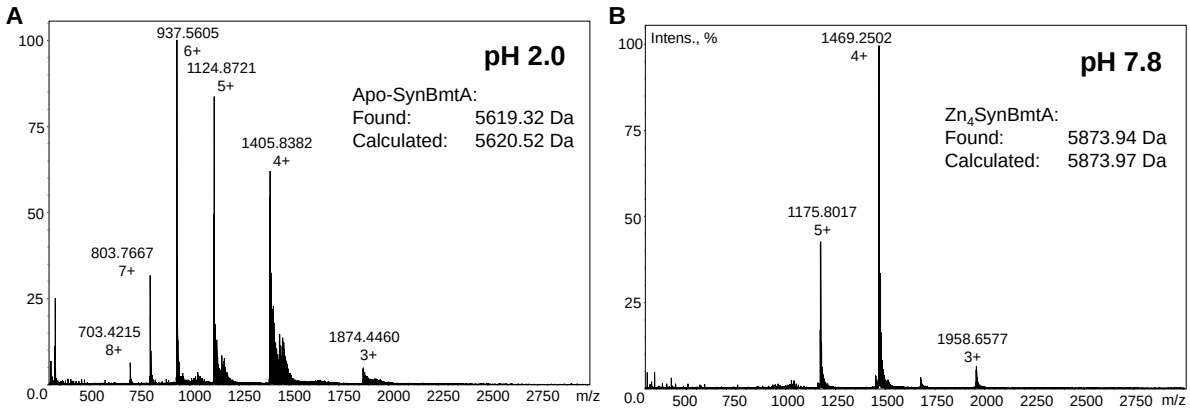

Figure 1. ESI-MS of BmtA. **A.** At pH 2 (10 µM protein, 20 mM NH_4HCO_3, 2% (v/v) HCOOH). The additional peaks at higher m/z values than the main species are mainly sodium adducts. **B.** At pH 7.8 (10 µM protein, 20 mM NH_4HCO_3).

At neutral pH, metallothioneins may be observed in their metallated form(s) [42-48]. A full ESI-MS spectrum of SynBmtA as purified, at pH 7.8, is shown in Figure 1B. Essentially, a single metallospecies was observed, with a mass in excellent agreement for that expected for a species containing 4 Zn^{2+} ions (Figure 1B). The identity of the bound metal ions was confirmed by Inductively-Coupled Plasma-Optical Emission Spectroscopy (ICP-OES). The only metal found at significant levels was zinc, with a SynBmtA:Zn ratio of 1:4.6±0.5 (Supplementary Table S2).

The amino acid sequence of SynBmtA is 34.5% identical (47.4% similar) to that of SmtA from freshwater *Synechococcus elongatus* sp. PCC 7942, the prototype BmtA for which a structure is available [10] (Figure 2B). The first seven zinc-binding residues, *i.e.* six cysteines and one histidine residue, are fully conserved. Other notable (semi-)conserved residues include several that form part of short β-strands (blue arrows in Figure 2B). All of these residues reside within the previously described zinc-finger portion of BmtAs [9,10,12,49]. To further test whether SynBmtA indeed adopts a similar fold to SmtA, Zn_4SynBmtA was subjected to solution NMR spectroscopy, enabling a partial sequential assignment (Figure 2A and Supplementary Table S3). Whilst a complete structural determination of SynBmtA was beyond the scope of the present study, chemical shift (Figure 2C) and NOE (Supplementary Figure S3) data reveal several hallmarks characteristic of the SmtA zinc-finger fold for residues Ala3-His37. Figure 2C compares the deviation of Hα proton NMR shifts from the calculated random coil shifts of SynBmtA and SmtA for assigned residues, using the alignment shown in Figure 2B. Deviations from random coil shifts are, amongst other influences, associated with secondary structure [50]. For the residues up to His37, there are clear similarities in the trends observed, including low-field shifts for the majority of residues expected to form β-strands (blue arrows in Figure 2B), and consistent high-field deviations starting at residue Thr31 that coincide with the short (4-5 residues) α-helix (red cylinder) present in SmtA [10] and PflQ2 MT [11]. NH-NH cross-peaks expected for a β-hairpin structure for residues Ile21 to Phe28 are also present (Supplementary Figure S3). There is also an NH-NH cross-peak between Ile4 and Val15; this is indicative of the formation of a β-bridge between these residues as seen in SmtA, where the two NH protons of Val7 and Val18 are at a distance of 3.7 Å (Supplementary Figure S3).

The chemical shift of the Hα proton of Ser34 is particularly noteworthy. Its extreme high-field shift (1.68 ppm) mirrors that for the corresponding Ala37 in SmtA (1.73 ppm) [10]. This has been attributed to a CH-π interaction between this proton and the aromatic ring of Tyr31, which stabilises the mutual orientation of the β-hairpin and the α-helix. The corresponding residue in SynBmtA is Phe28. Interestingly, the hydroxy group seems to have "jumped" between these residues. A final hallmark for the zinc-finger fold is the extreme low-field shift of the NH proton of Cys29 (10.14 ppm). In SmtA, the corresponding NH of Cys32 (10.09 ppm) forms an NH-S hydrogen bond to the thiolate sulfur of Cys9 [10]. Both residues are part of the "zinc-finger" site A. Meanwhile, this feature has been observed in several other bacterial MTs, including those from *Pseudomonas aeruginosa* and *Pseudomonas putida* [12], as well as that from *Pseudomonas fluorescens* [11]. The proximity of residues forming zinc site A is further confirmed by inter-residue NOESY cross-peaks

between backbone NH and Hβ protons of Cys6, Cys29 and Cys33 (Supplementary Figure S3). All of these observations are represented in the homology model shown in Figure 2D.

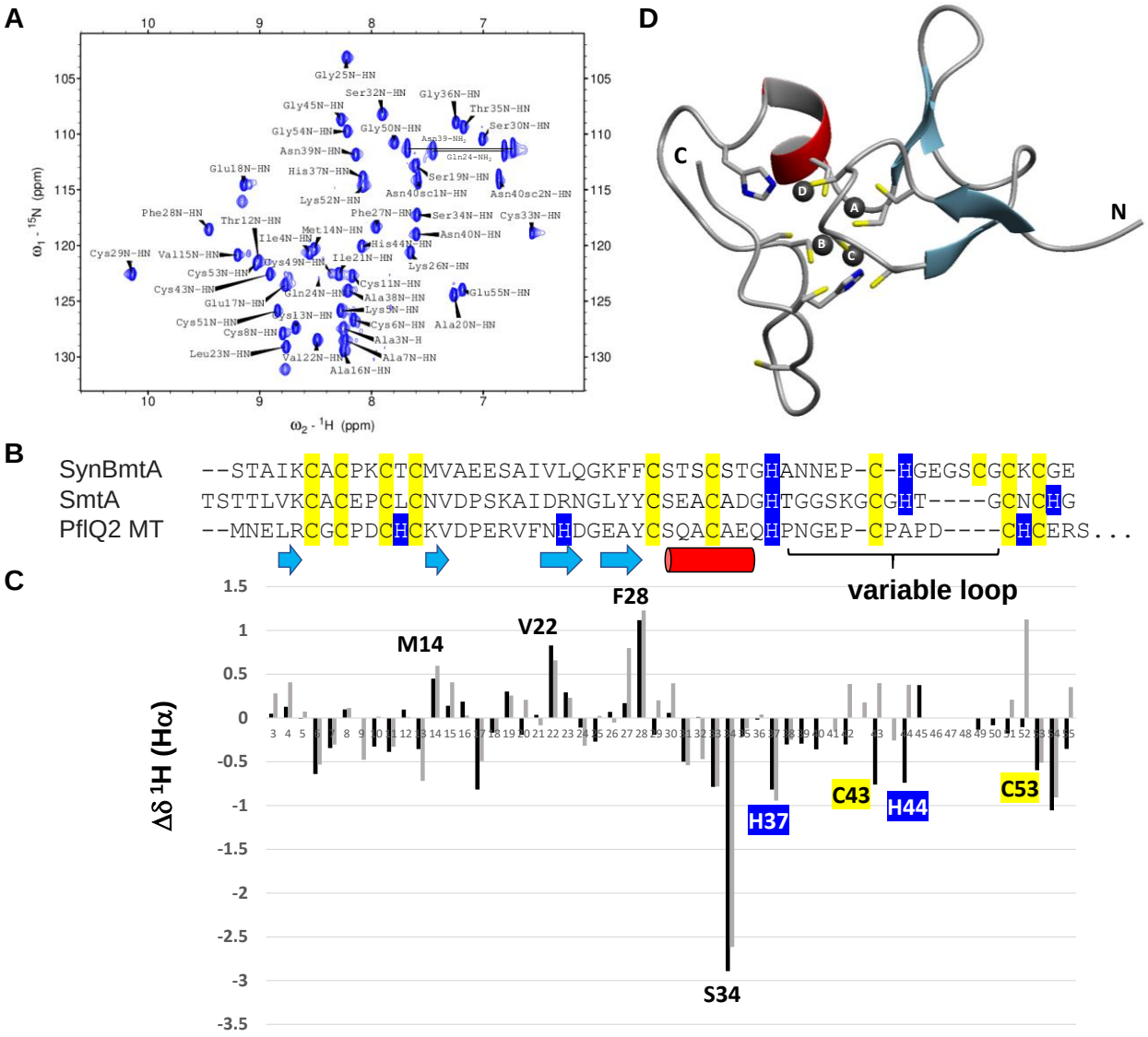

Figure 2. SynBmtA adopts the typical zinc finger fold but differs from other bacterial MTs in the C-terminal portion. **A.** [^{1}H,^{15}N] HSQC spectrum illustrating sequential assignment of Zn_4SynBmtA. **B.** Sequential alignment of SynBmtA with SmtA from *Synechococcus elongatus* strain PCC 7942 [12] and P*seudomonas fluorescens* Q2-87 MT [11]. **C.** Comparison of deviations from calculated random coil shifts [50] for Hα protons of SynBmtA (black) and SmtA (grey). The comparison is based on the alignment shown in Figure 2B. Alternative alignments lead to larger differences between SmtA and SynBmtA for the C-terminal cysteines. **D.** Homology model of SynBmtA, with Zn_4SmtA (pdb 1jjd) and the truncated A44H mutant of Cd-PflQ2 MT (pdb 6gv7) as templates, using the alignment shown in Figure 2B. The zinc ions (black) are labelled as in SmtA (pdb 1jjd). C- and N-terminus are indicated.

The structure of the remaining 18 C-terminal residues cannot be predicted reliably. Previously, the portion between the conserved His residue (His40 in SmtA) and the last pair of Cys residues (Cys52 and Cys54 in SmtA) has been termed the "variable loop" [49], as it is characterised by very low sequence similarity

between BmtAs from different species, as is also evident from Figure 2B. This would inherently hamper structure prediction by homology modelling. In addition, residues Glu41, Pro42, Glu46, Gly47 and Ser48 of SynBmtA could not be assigned; we note that a similar situation had been encountered with SmtA, where residues Gly42, Gly50, and Thr51 also remained unassigned. The respective loop is likely flexible and solvent-exposed [10], and this appears to be the case for SynBmtA as well. Finally, SynBmtA possesses an additional Cys residue with metal-binding potential: instead of the more common CxC pair, SynBmtA (and many related BmtAs from other *Synechococcus* strains; Supplementary Table S4) has a CxCxC motif – and in each case, this coincides with a PCH motif instead of the more common CxH motif for Cys47 and His49 in SmtA. It is *a priori* unclear which of the two CxC pairs in this motif should be aligned with the single CxC motif in SmtA. The sequential alignment in the C-terminal part in Figure 2B is based on comparing the chemical shift index data displayed in Figure 2C, where a closer match was obtained for the alignment as shown. Ultimately, this alignment also results in a metal-ligand connectivity pattern that corresponds to a $Zn_4Cys_9His_2$ cluster as observed for SmtA [12], with both His37 and His44 participating. The drawback of the model resulting from this alignment (Figure 2D) is that Cys49 then forms part of an extended loop, in a position that is too far away from other Cys residues or modelled metal ions. Models using alternative alignments (not shown) lead to Cys53 too far away to participate in metal binding. In either case, non-coordinating Cys residues in a flexible loop (or at the C-terminal end) that do not participate in metal binding seem unlikely. It is therefore clear that other cluster compositions are not only possible but likely, including a $Zn_4Cys_{10}His$ (involving Cys49 but not His44) and a $Zn_4Cys_{10}His_2$ cluster (involving all 12 Cys and His residues). Although rare, there is at least one example in the literature where an M_4L_{12} cluster has been observed [51]. Furthermore, a similar situation as in PflQ2 MT, where further alternative binding modes have been discussed [11], is in principle also possible.

In summary, a reliable structure prediction was possible for the zinc finger portion of SynBmtA. In contrast, limited NMR data and the lack of sequence similarity for the C-terminal region means that the structure of this region, or the full topology of the metal cluster, could not be determined or predicted reliably with the available published structures and data.

3.2. The zinc-binding affinity of SynBmtA exceeds that of other MTs

A major goal for the present work was to pave the way for investigating the ternary system consisting of SynZur, SynBmtA and Zn^{2+}. In preparation to address this objective, knowledge of the zinc-binding affinities of the two proteins is desirable. The affinity of the sensory site in SynZur was determined recently [24] by spectrophotometric titrations using Quin-2 as competitive zinc chelator and metallochromic reporter; this approach has previously given reliable binding constants for other zinc sensors [52,53] including Zur proteins [23]. SynZur was expressed and purified in its fully metallated form, which is predominantly dimeric ($(Zn_2SynZur)_2$). The sensory zinc ion can be conveniently removed from $Zn_2SynZur$ by treatment with excess

EDTA, leaving the second (structural) zinc ion untouched [24], as observed for other Fur-family proteins (Supplementary Figure S4). Titrating the resulting Zn_1SynZur preparation with zinc in the presence of a slight excess of Quin-2 (Supplementary Figure S4), and fitting the data using a simple 1:1 binding model gave K_D = (8.3±2.5)x10^{-13} M, a value in a range similar to that of other Zur sensors [54-56].

To ensure comparability of the affinity data, we wished to use the same approach for SynBmtA, which required the preparation of apo-SynBmtA. Many other MTs have been shown to readily release their metal ions to EDTA [36]. This includes SmtA, which can be completely demetallated using a small excess of EDTA over total Zn, and also reacts quantitatively with larger excesses within a few hours [57]. Unexpectedly, the reaction of SynBmtA with a 100-fold excess of EDTA under comparable conditions was not completed even after 24 h, and closer inspection of the reaction products revealed that the apo-protein generated was largely oxidised (Supplementary Figure S5). The chelator TPEN (K_D(pH 7.4) = 6.4×10^{-16} M), which has a higher zinc affinity than EDTA (K_D (pH 7.4) = 2.3×10^{-14} M) at physiological pH [58], in the presence of the reducing agent DTT, was not able to remove any zinc from SynBmtA either. We note that this resistance to react with small-molecule chelators would also preclude the determination of zinc affinity by competition with the chelator 5F-BAPTA, another approach that has been used to assess metal-binding affinity of many other MTs [36]. Even the addition of the denaturant urea (6 M) did not generate the desired apo-protein (Supplementary Figure S5) – indicating that the protein was extremely stably folded. Since at this stage it was unclear whether the resistance against zinc release was due to kinetic effects, such as low accessibility of the zinc ions, or unfavourable electrostatic interactions, we determined the pH of half-displacement ($pH_{1/2}$) for SynBmtA. This value, often also referred to as apparent pK_a [59], is routinely used to characterise MTs [36]. It can be readily determined from spectrophotometric pH titrations, monitoring the thiolate-to-metal charge transfer bands [60]. The $pH_{1/2}$ of Zn_4SynBmtA in 20 mM NH_4HCO_3 was 3.94±0.04 (Figure 3A). To the best of our knowledge, this is the lowest $pH_{1/2}$ ever determined for a Zn-MT, with values reported to range from 4.1 up to 5.4 for MTs from a variety of species [59]. The record for the lowest value, broadly signifying highest affinity, was previously held by SmtA [10,61].

Nonetheless, the pH titration as well as the ESI-MS spectrum of SynBmtA at pH 2 (Figure 1A) indicate that complete zinc release does occur at sufficiently low pH. Therefore, under strict exclusion of oxygen, zinc was removed by gel filtration at low pH [62], followed by buffer-exchange into 20 mM NH_4HCO_3 (pH 7.8), also using a gel filtration column. This yielded fully reduced, soluble apo-SynBmtA (Figure 3B, upper panel). Most importantly, addition of four molar equivalents of Zn^{2+} to this preparation gave Zn_4SynBmtA as the sole metallospecies, with no indication for oxidation or other heterogeneity beyond the formation of potassium adducts in the ESI-MS spectrum (Figure 3B, bottom).

With a viable approach to generate apo-SynBmtA to hand, it was then possible to carry out the titration with Zn^{2+} in the presence of Quin-2 as for Zn_1SynZur. This gave K_D(Zn-SynBmtA) = (1.13±0.07)×10^{-14} M, corresponding to an apparent binding constant of log K' = 13.9 (binding constants are more common in the

MT literature, so this will be used for further comparisons). However, only few data points are on the curved portion of the plot, which means that there was little competition from Quin-2, and that the determined K_D may be over-estimated (and log *K*' underestimated). We further note that this binding constant refers to the average over all four binding sites, as is, with very few exceptions, common for affinity data for MTs [36]. Furthermore, the ionic strength (*I* = 0.02 M) in all of our experiments is relatively low. Low ionic strength increases the stability of metal complexes including that of MTs [49,36]. However, the apparent log *K*' for wild-type SmtA at even lower *I* = 0.004 M and pH 8.1 was *ca.* 13, *i.e.* still nearly an order of magnitude lower [49]. Since SmtA thus had, up until now, displayed the highest apparent affinity constant measured for an MT, it is clear that SynBmtA, with an at least 10-fold higher affinity still, breaks this record, also consistent with the lowest $pH_{1/2}$ we have determined.

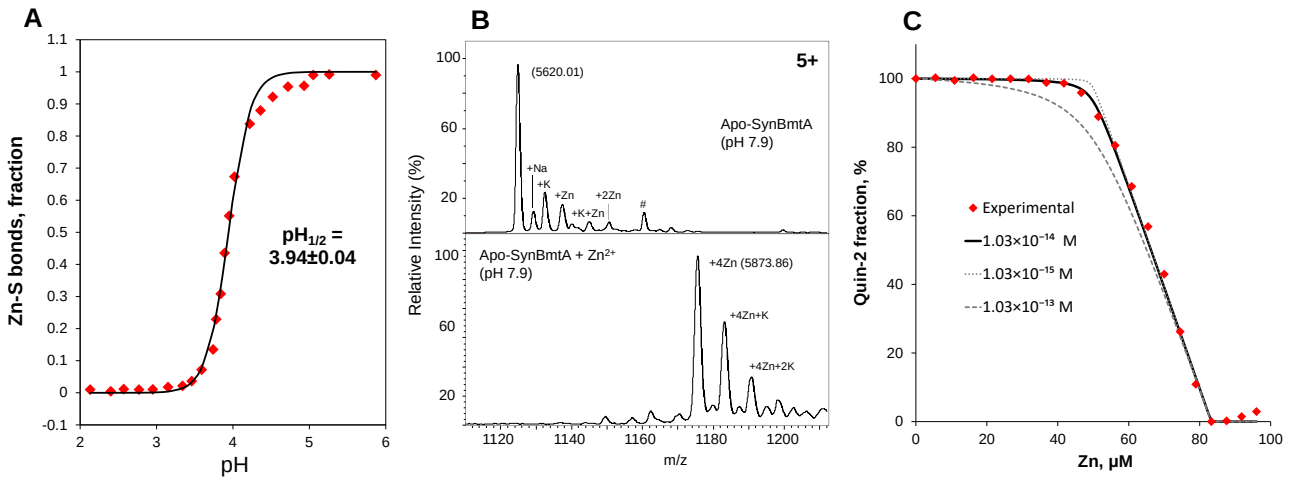

Figure 3. High Zn affinity of SynBmtA. **A.** Determination of $pH_{1/2}$ (20 µM SynBmtA, 20 mM NH_4HCO_3). Absorbance was measured at 230 nm; the plotted values are the result of subtracting the absorbance at pH 2.1 (assumed to correspond to absorbance from apo-protein) from the readings at all other pH values. The black solid line corresponds to a curve fit. **B.** Successful generation of apo-SynBmtA (upper panel) at pH 7.8 (see main text; 10 µM SynBmtA, 20 mM NH_4HCO_3). The lower panel demonstrates that the protein prepared in this way is capable of regenerating the native Zn_4SynBmtA holo-protein. The +5 charge state is shown. The potassium adducts derive from usage of a pH electrode to adjust buffer pH. **C.** Representative titration of apo-SynBmtA (12.4 µM protein = 49.6 µM binding sites) with Zn^{2+}, in presence of 33.7 µM Quin-2. Free Quin-2 was monitored through absorbance at 261 nm. The solid line corresponds to a fit to a 1:1 model with the indicated K_D; the dotted and the dashed lines describe models with 10-fold higher and lower affinity, respectively. The average K_D from triplicate measurements was $(1.13\pm0.07)\times10^{-14}$ M.

The apparent binding constant we have determined for SynBmtA (log *K*' = 13.9) is over an order of magnitude lower than that for TPEN (log *K*' = 15.2), and similar to that for EDTA (13.7). The latter values are valid for *I* = 0.1 M and pH 7.4 [58]; thus the actual values for EDTA and TPEN at *I* = 0.02 M and pH 7.8 will be even higher. So thermodynamically, a 100-fold excess of either chelator really should be sufficient to extract a substantial amount of zinc from SynBmtA. Since this was not observed, we conclude that the lack of reactivity must be

due to kinetic effects, e.g. the inaccessibility of the zinc ions in SynBmtA. The 2nd-order kinetics observed previously for reactions between metallated MTs and EDTA [57,63], as well as respective adducts observed in ESI-MS experiments monitoring such reactions [40] support the notion that zinc transfer requires direct contact between protein and chelator – in essence the formation of a transient ternary complex. It would appear that this does not occur in the case of SynBmtA.

Previous work has indicated that the most accessible and hence most reactive zinc site in SmtA is site C [43]. This site encompasses Cys16, Cys32, Cys47 and His49. The oxidised Zn_3 form of the His49Cys mutant, where a disulfide bridge can be formed between Cys16 and Cys49 when site C is not occupied by Zn^{2+}, was completely unreactive towards EDTA, highlighting the importance of this site for metal-transfer reactions [57]. Site C is also the site most affected by differences in the variable loop (Figure 2B and ref. 49). It is therefore likely that the lack of reactivity of SynBmtA is at least in part attributable to the structure around site C. Although we were unable to resolve the structure of this region, it is evident that it will differ from the respective region in SmtA. It is also likely to play a role in the enhanced stability of the metal cluster, but other effects including more subtle differences in electrostatics may also contribute.

3.4. SynBmtA can remove Zn from SynZur

SynZur binds, in its fully metallated form (Zn:SynZur = 2:1; Supplementary Figure S4), to the promoter region of the *synbmtA* gene with an affinity below 100 nM (Figure 4A, top), activating *synbmtA* transcription [24]. The DNA-binding affinity of EDTA-treated SynZur (Zn:Zur = 1:1; Supplementary Figure S4) is markedly decreased (Figure 4A, bottom). This means that as long as fully metallated SynZur is bound to DNA, production of SynBmtA will continue, and the newly produced MT will pick up any Zn^{2+} that exceeds the buffered intracellular concentration that is appropriate for *Synechococcus* sp. WH8102. At some stage, when the bacterium is no longer in a zinc-rich environment and the intracellular concentration is in the ideal range, activation of transcription will need to be turned off, which requires the absence of the ternary Zn-SynZur-DNA complex. Although dissociation of this metallosensor-DNA complex is not the only plausible pathway for SynZur deactivation, we were curious whether apo-SynBmtA would be able to extract Zn^{2+} from metallated SynZur, as would be expected from the MT's much higher Zn^{2+}-binding affinity ($K_D \leq (1.13\pm0.07)\times10^{-14}$ M vs. $(8.3\pm2.5)\times10^{-13}$ M).

For this proof-of concept study, a mixture of Zn_2SynZur and apo-SynBmtA was incubated for 30 min and then subjected to native ESI-MS at pH 7.8. A section from the resulting spectrum is shown in Figure 4B, together with the same section from spectra run for the isolated proteins from the same batches as used in the reaction. The spectrum of the mixture indicates the generation of Zn_1SynZur, together with a decrease in the relative intensity of Zn_2SynZur (Figure 4B; both monomeric and dimeric SynZur were observed in the spectra; see Supplementary Figure S6 for a representative dimeric charge state). There was no indication of

completely Zn-free SynZur. In turn, the intensity of apo-SynBmtA decreased significantly, with the major species emerging being Zn_1SynBmtA. Small amounts of Zn_2SynBmtA were also apparent.

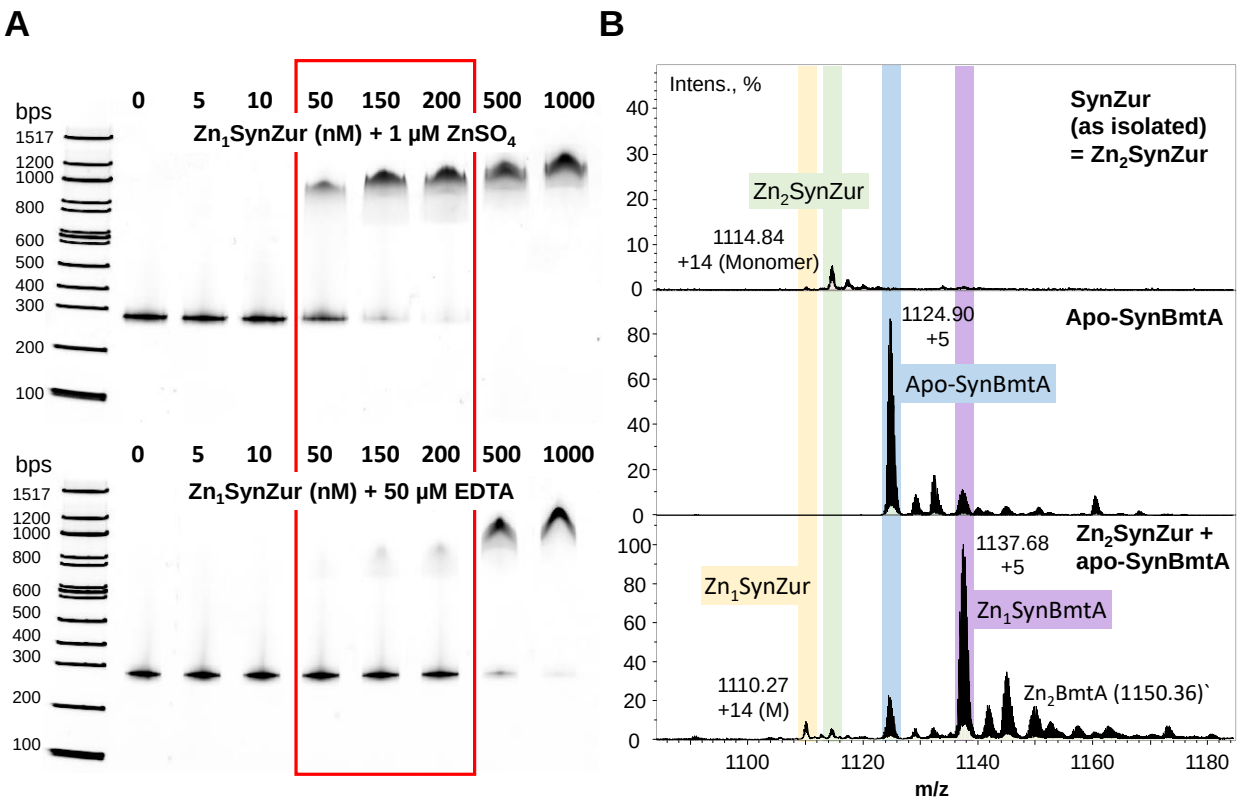

Figure 4. Removal of sensory zinc from SynZur by SynBmtA. **A.** EMSAs of metallated (top) and EDTA-treated SynZur (bottom) binding to the *synbmtA* promoter (250 bp; Supplementary Figure S2; 5 ng in each lane). The lower band in both gels corresponds to free promoter DNA; the higher bands correspond to SynZur:DNA complexes. The red box highlights the concentration range where the differences between fully metallated and EDTA-treated SynZur (= mono-metallated Zn_1SynZur) are most evident. The additional EDTA in the mixtures is added as a safeguard against re-metallation by background Zn^{2+} that may be present in the gel or buffer. **B.** Representative sections of ESI-MS spectra of native Zn_2SynZur (top), apo-SynBmtA (middle), and a mixture of the two proteins (bottom) (20 µM SynZur and 5 µM BmtA; 20 mM NH_4HCO_3, pH 7.8). The section shown displays the +14 charge state of monomeric SynZur, and the +5 charge state of BmtA. The differences in intensities between the two proteins stem from different ionisation efficiencies, with the larger SynZur yielding fewer gas phase ions across the entire spectrum, despite being present in excess. Note that it is also not straightforward to derive quantitative information from native ESI-MS spectra, as this would require summing up all species present in the spectra, with monomeric and dimeric species having very different ionisation efficiencies.

Crucially, under the conditions and within the timeframe employed, this experiment demonstrates that apo-BmtA is able to extract zinc from Zn_2SynZur (or $(Zn_2SynZur)_2$; see Supplementary Figure S6). We suggest that the more labile sensory site is the origin of the transferred zinc, and that the remaining zinc in Zn_1SynZur is bound to the structural site that is also not reactive towards EDTA (Supplementary Figure S4). It is plausible

to suggest that *in vivo*, production of excess apo-SynBmtA could disrupt SynZur-DNA complexes and hence de-activate the transcription of the *synbmtA* gene.

Clearly, this pilot experiment opens opportunities for extensive future investigations, including product analysis after longer reaction times, testing whether reaction with apo-SynBmtA abolishes the DNA binding ability of SynZur, and whether apo-SynBmtA is also capable of removing zinc from SynZur-DNA complexes – as previously observed for mammalian MT and transcription factor IIIa [64].

4. Discussion

We have characterised the bacterial MT from *Synechococcus* sp. WH8102, and two different approaches indicated that it has higher zinc-binding affinity than any previously characterised MT. Assuming that the K_D's of MTs are in some way linked to intracellular buffered zinc concentrations, the higher stability of (cyano-)bacterial MTs compared to eukaryotic MTs may be related to bacteria having to deal with lower intracellular zinc levels [65]. The further increase in affinity from SmtA to SynBmtA may reflect the lower zinc requirements of the open ocean strain WH8102 compared to freshwater *Synechococcus*. The divergent C-terminus likely plays a role in this increased affinity. Analysis of a multiple sequence alignment of BmtA sequences deposited in the non-redundant protein database at NCBI (Supplementary Table S4) revealed that BmtAs which harbour both the PCH and the CxCxC motif in their C-terminal portions occur in *Synechococcus* species across a range of clades from subcluster 5.1, but also in *Cyanobium* spp. and the euryhaline *Synechococcus* sp. WH5701, both of which belong to subcluster 5.2. In addition, the freshwater species *Aphanothece minutissima* BmtA also displays these features. There is therefore no obvious correlation between ecological niche and prevalence of these sequence features.

Comparing the zinc affinities of SynBmtA and the zinc sensor that regulates its expression revealed that the affinity of the MT is significantly higher than that of the sensor – a situation also encountered for mammalian MTs and their regulator MTF-1, which has regulatory binding sites with relatively weak affinity [66]. The difference in affinities between MT and sensor prompted us to investigate whether SynBmtA is able to abstract zinc from the sensory sites of SynZur, and we could show that this is indeed the case, after a relatively short reaction time. It remains to be seen whether this reaction requires direct protein-protein interaction.

The purpose of metallosensors is to ensure that the cytosolic buffered concentration of a given metal ion remains within a narrow range. The dissociation constants for the metal-sensor complexes are generally closely associated with these concentrations [65]. Many bacteria harbour both "scarcity" and "excess" sensors – for example, *E. coli* employs Zur to upregulate zinc import through ZnuABC during zinc scarcity, and ZntR to upregulate zinc export through the ZntA ATPase [67]. Similarly, freshwater cyanobacteria have Zur to regulate ZnuABC, and SmtB-like sensors to regulate either export (AztA, BxmA) or storage (SmtA) [18].

Synechococcus sp. WH8102 harbours a single zinc sensor that regulates both uptake (by (de-)repression of *znuABC*) and storage (by activation of *synbmtA*) [24]. The fact that the storage protein has considerably higher zinc affinity than the activating sensor raises an interesting question: What is the optimal buffered concentration of zinc in the WH8102 cytosol? Is it set to the affinity of SynBmtA or to that of the sensor? Here, it is especially pertinent to highlight that we have observed appreciable expression of *synbmtA* under basal conditions (*i.e.* in the absence of excess zinc) [24]. Significantly, *znuABC* was still partially repressed under these conditions, suggesting that SynZur had access to sufficient zinc to populate its sensory binding site – *i.e.* any SynBmtA present did not out-compete all SynZur molecules present. This would ultimately suggest that the intracellular concentration is set by the sensor as usual. Future work will need to measure the *in vivo* protein concentrations of both sensor and metallothionein to start building up a quantitative framework for zinc homeostasis in this and other oligotrophic marine cyanobacteria.

Perhaps the most fundamental question is why WH8102 harbours an MT at all – what advantage does this gene confer, and how do the properties characterised here fit into this? We firstly note that SynBmtA is upregulated at elevated [Zn^{2+}], consistent with a role in protecting against zinc toxicity. This also implies that SynZur is not only a sensor of zinc depletion (via upregulation of the *znuABC* uptake system [24]), but also of zinc excess. However, the fact that an MT is used rather than an efflux pump may indicate that for this strain, zinc is a valuable resource worth retaining. The fact that *synbmtA* expression is regulated by [Zn^{2+}] suggests that zinc availability is subject to changes in the ecological niche inhabited by WH8102. Indeed, WH8102 was first isolated from the Sargasso Sea. Even though this has previously been considered as somewhat of an ocean desert, more recent work has shown that there is episodic nutrient (including zinc) input from deeper layers via mesoscale eddies, currents that promote mixing of different seawater layers [68]. The huge variations in cellular zinc quotas in *Synechococcus* encountered in field samples from such eddies [26] are likely enabled by variations in zinc-dependent *bmtA* expression. Thus, WH8102 and related strains of clade III that also harbour *bmtA* genes [24] are well adapted to cope with significant changes in zinc availability, with BmtA facilitating survival at both elevated and scarce [Zn^{2+}]. A related aspect concerns the fact that surface waters of the Sargasso Sea and other habitats of clade III strains are extremely depleted for phosphorus. Parallels in expression patterns of *synbmtA* and a predicted phosphatase have been noted [28], leading to the suggestion that SynBmtA might have a role in supplying zinc to this enzyme. One question that remains is how such enzymes would acquire zinc stored in SynBmtA. Although there are several studies demonstrating zinc transfer from metallated MTs to enzymes [69] including alkaline phosphatase [70], a direct transfer from SynBmtA to other proteins seems unlikely, given the kinetic inertness observed with the smaller zinc acceptors EDTA and TPEN. Furthermore, any mechanism involving the full dissociation of Zn^{2+} ions would have much too slow kinetics to allow for efficient metal transfer [71]. If the zinc stored in SynBmtA can, eventually, be utilised to metallate zinc-requiring proteins, a notion that makes overall biological sense, we hypothesise that this would involve either oxidative [72] or proteolytic [73,74] processes.

5. Conclusions

Although metallothioneins have remained a relatively rare occurrence in bacteria, many cyanobacterial strains produce these intriguing proteins, predominantly to deal with zinc [9]. It has previously been speculated that the variations in primary structure seen for BmtAs from different strains may relate to their habitat [49], and SynBmtA from *Synechococcus* sp. WH8102 supports this idea: the strain inhabits areas of the ocean that are extremely low in most nutrients including zinc, and its single metallothionein displays the highest zinc affinity recorded for an MT so far. It is interesting to note that the coastal strain *Synechococcus* sp. CC9311 harbours no less than four different *bmtA* genes [49], one of which (*sync1081*) is closely related to SynBmtA studied in this work, and indeed also harbours a Zur box in its promoter region [24]. In contrast, the other three *bmtA* genes are not predicted to be Zur-regulated. This raises the question whether BmtAs have roles beyond zinc homeostasis, such as protection against oxidative stress as seen for MTs from other organisms [3]. Ultimately, we would like to further our understanding whether harbouring MT genes provides advantages in terms of which ecological niches are accessible to these strains.

Acknowledgements

This work was supported by the University of Warwick via a Chancellor's International Scholarship to A.M We thank Dr. Lijiang Song for supporting inorganic and molecular mass spectrometry experiments and Dr. Ivan Prokes for supporting NMR experiments. We also thank the Brilliant Club and the Nuffield Foundation for supporting a research placement for Harry Fyjis-Walker. This work was supported by the Natural Environment Research Council (grant reference NE/I00985X/1). Some equipment used in this research was obtained through Birmingham Science City with support from Advantage West Midlands and the European Regional Development Fund.

References

1. Margoshes, M.; Vallee, B. L., A cadmium protein from equine kidney cortex. *J. Am. Chem. Soc.* **1957,** *79* (17), 4813-4814.
2. Binz, P. A.; Kägi, J. H. R., *Metallothionein: Molecular evolution and classification*. Birkhäuser Verlag AG: Basel, 1999; p 7-13.
3. Blindauer, C. A.; Leszczyszyn, O. I., Metallothioneins: unparalleled diversity in structures and functions for metal ion homeostasis and more. *Nat. Prod. Rep.* **2010,** *27* (5), 720-741.
4. Guirola, M.; Naranjo, Y.; Capdevila, M.; Atrian, S., Comparative genomics analysis of metallothioneins in twelve *Drosophila* species. *J. Inorg. Biochem.* **2011,** *105* (8), 1050-1059.
5. Olafson, R. W.; Abel, K.; Sim, R. G., Prokaryotic metallothionein - preliminary characterization of a blue-green-alga heavy metal-binding protein. *Biochem. Biophys. Res. Commun.* **1979,** *89* (1), 36-43.
6. Higham, D. P.; Sadler, P. J.; Scawen, M. D., Cadmium-resistant *Pseudomonas putida* synthesizes novel cadmium proteins. *Science* **1984,** *225*, 1043-1046.
7. Schmidt, A.; Hagen, M.; Schütze, E.; Schmidt, A.; Kothe, E., In silico prediction of potential metallothioneins and metallohistins in actinobacteria. *J. Basic Microbiol.* **2010,** *50* (6), 562-569.
8. Blindauer, C. A., Bacterial metallothioneins. In *Metal Ions in Life Sciences*, Sigel, A.; Sigel, H.; Sigel, R. K. O., Eds. 2009; Vol. 5, pp 51-81.
9. Blindauer, C. A., Bacterial metallothioneins: past, present, and questions for the future. *J. Biol. Inorg. Chem.* **2011,** *16* (7), 1011-1024.
10. Blindauer, C. A.; Harrison, M. D.; Parkinson, J. A.; Robinson, A. K.; Cavet, J. S.; Robinson, N. J.; Sadler, P. J., A metallothionein containing a zinc finger within a four-metal cluster protects a bacterium from zinc toxicity. *Proc. Natl. Acad. Sci. USA* **2001,** *98* (17), 9593-9598.
11. Habjanic, J.; Zerbe, O.; Freisinger, E., A histidine-rich *Pseudomonas* metallothionein with a disordered tail displays higher binding capacity for cadmium than zinc. *Metallomics* **2018,** *10* (10), 1415-1429.
12. Blindauer, C. A.; Harrison, M. D.; Robinson, A. K.; Parkinson, J. A.; Bowness, P. W.; Sadler, P. J.; Robinson, N. J., Multiple bacteria encode metallothioneins and SmtA-like zinc fingers. *Mol. Microbiol.* **2002,** *45* (5), 1421-1432.
13. Morby, A. P.; Turner, J. S.; Huckle, J. W.; Robinson, N. J., SmtB is a metal-dependent repressor of the cyanobacterial metallothionein gene *smtA*: Identification of a Zn inhibited DNA-protein complex. *Nucleic Acids Res.* **1993,** *21* (4), 921-925.
14. Liu, T.; Nakashima, S.; Hirose, K.; Uemura, Y.; Shibasaka, M.; Katsuhara, M.; Kasamo, K., A metallothionein and CPX-ATPase handle heavy-metal tolerance in the filamentous cyanobacterium *Oscillatoria brevis*. *FEBS Lett* **2003,** *542* (1-3), 159-63.
15. Divya, T. V.; Chandwadkar, P.; Acharya, C., NmtA, a novel metallothionein of *Anabaena* sp. strain PCC 7120 imparts protection against cadmium stress but not oxidative stress. *Aquat. Toxicol.* **2018,** *199*, 152-161.
16. Turner, J. S.; Morby, A. P.; Whitton, B. A.; Gupta, A.; Robinson, N. J., Construction of Zn^{2+}/Cd^{2+} hypersensitive cyanobacterial mutants lacking a functional metallothionein locus. *J. Biol. Chem.* **1993,** *268* (6), 4494-4498.
17. Liu, T.; Golden, J. W.; Giedroc, D. P., A zinc(II)/lead(II)/cadmium(II)-inducible operon from the cyanobacterium *Anabaena* is regulated by AztR, an alpha 3N ArsR/SmtB metalloregulator. *Biochemistry* **2005,** *44* (24), 8673-8683.
18. Blindauer, C. A., Zinc handling in cyanobacteria - an update. *Chem. Biodiv.* **2008,** *5*, 1990-2013.
19. Scanlan, D. J.; Ostrowski, M.; Mazard, S.; Dufresne, A.; Garczarek, L.; Hess, W. R.; Post, A. F.; Hagemann, M.; Paulsen, I.; Partensky, F., Ecological genomics of marine picocyanobacteria. *Microbiol. Mol. Biol. Rev.* **2009,** *73* (2), 249-299.
20. Barnett, J. P.; Millard, A.; Ksibe, A. Z.; Scanlan, D. J.; Schmid, R.; Blindauer, C. A., Mining genomes of marine cyanobacteria for elements of zinc homeostasis. *Front. Microbiol.* **2012,** *3*, 142.

21. Dore, H.; Farrant, G. K.; Guyet, U.; Haguait, J.; Humily, F.; Ratin, M.; Pitt, F. D.; Ostrowski, M.; Six, C.;Brillet-Gueguen, L.; Hoebeke, M.; Bisch, A.; Le Corguille, G.; Corre, E.; Labadie, K.; Aury, J. M.; Wincker, P.; Choi, D. H.; Noh, J. H.; Eveillard, D.; Scanlan, D. J.; Partensky, F.; Garczarek, L., Evolutionary mechanisms of long-term genome diversification associated with niche partitioning in marine picocyanobacteria. *Front. Microbiol.* **2020,** *11*, 23.
22. Hantke, K., Bacterial zinc uptake and regulators. *Curr. Opin. Microbiol.* **2005,** *8* (2), 196-202.
23. Mikhaylina, A.; Ksibe, A. Z.; Scanlan, D. J.; Blindauer, C. A., Bacterial zinc uptake regulator proteins and their regulons. *Biochem. Soc. Trans.* **2018,** *46*, 983-1001.
24. Mikhaylina, A.; Ksibe, A. Z.; Wilkinson, R, C.; Smith, D.; Marks, E.; Coverdale, J. P. C.; Fülöp, V.; Scanlan, D. J.; Blindauer, C. A, A single sensor controls large variations in zinc quotas in a marine cyanobacterium, *under review*.
25. Shi, J. G.; Lindsay, W. P.; Huckle, J. W.; Morby, A. P.; Robinson, N. J., Cyanobacterial metallothionein gene expressed in *Escherichia-coli* - metal-binding properties of the expressed protein. *FEBS Lett.* **1992,** *303* (2-3), 159-163.
26. Twining, B. S.; Nunez-Milland, D.; Vogt, S.; Johnson, R. S.; Sedwick, P. N., Variations in *Synechococcus* cell quotas of phosphorus, sulfur, manganese, iron, nickel, and zinc within mesoscale eddies in the Sargasso Sea. *Limnol. Oceanogr.* **2010,** *55* (2), 492-506.
27. Palenik, B.; Brahamsha, B.; Larimer, F. W.; Land, M.; Hauser, L.; Chain, P.; Lamerdin, J.; Regala, W.; Allen, E. E.; McCarren, J.; Paulsen, I.; Dufresne, A.; Partensky, F.; Webb, E. A.; Waterbury, J., The genome of a motile marine *Synechococcus*. *Nature* **2003,** *424* (6952), 1037-1042.
28. Cox, A. D.; Saito, M. A., Proteomic responses of oceanic *Synechococcus* WH8102 to phosphate and zinc scarcity and cadmium additions. *Front. Microbiol.* **2013,** *4*, 17.
29. Cox, A. D.; Noble, A. E.; Saito, M. A., Cadmium enriched stable isotope uptake and addition experiments with natural phytoplankton assemblages in the Costa Rica upwelling dome. *Mar. Chem.* **2014,** *166*, 70-81.
30. Wishart, D. S.; Bigam, C. G.; Yao, J.; Abildgaard, F.; Dyson, H. J.; Oldfield, E.; Markley, J. L.; Sykes, B. D. ^{1}H, ^{13}C and ^{15}N chemical shift referencing in biomolecular NMR. *J. Biomol. NMR* **1995**, 6 (2), 135–140.
31. Goddard, T. D.; Kneller, D. G. Sparky 3 - NMR assignment program. University of California: San Francisco, **2007**.
32. Kjaergaard, M.; Poulsen, F.M. Sequence correction of random coil chemical shifts: correlation between neighbor correction factors and changes in the Ramachandran distribution. *J. Biomol. NMR,* **2011***,* 50(2), 157-165.
33. Fiser, A.; Sali, A., Modeller: Generation and refinement of homology-based protein structure models. In *Macromolecular crystallography, Part d*, Carter, C. W.; Sweet, R. M., Eds. Elsevier Academic Press Inc: San Diego, **2003**; Vol. 374, pp 461-491.
34. Jefferson, J. R.; Hunt, J. B.; Ginsburg, A. Characterization of Indo-1 and Quin-2 as spectroscopic probes for Zn^{2+}-protein interactions. *Anal. Biochem.* **1990**, *187* (2), 328–336.
35. Kuzmič, P. Program DYNAFIT for the analysis of enzyme kinetic data: application to HIV proteinase. *Anal. Biochem.* **1996**, *237*, 260–273.
36. Blindauer, C. A., Chapter 21: Metallothioneins. In *Binding, transport and storage of metal ions in biological cells*, Maret, W.; Wedd, A. G., Eds. The Royal Society of Chemistry: Cambridge, UK, 2014; pp 606-665.
37. Kowald, G. R.; Stürzenbaum, S. R.; Blindauer, C. A., Earthworm *Lumbricus rubellus* MT-2: Metal binding and protein folding of a true cadmium-MT. *Int. J. Mol. Sci.* **2016,** *17* (1), 16.
38. M'Kandawire, E.; Mierek-Adamska, A.; Stürzenbaum, S. R.; Choongo, K.; Yabe, J.; Mwase, M.; Saasa, N.; Blindauer, C. A., Metallothionein from wild populations of the African catfish *Clarias gariepinus*: From sequence, protein expression and metal binding properties to transcriptional biomarker of metal pollution. *Int. J. Mol. Sci.* **2017,** *18* (7), 28.
39. Mierek-Adamska, A.; Dabrowska, G. B.; Blindauer, C. A., The type 4 metallothionein from *Brassica napus* seeds folds in a metal-dependent fashion and favours zinc over other metals. *Metallomics* **2018,** *10* (10), 1430-1443.

40. Imam, H. T.; Blindauer, C. A., Differential reactivity of closely related zinc(II)-binding metallothioneins from the plant *Arabidopsis thaliana*. *J. Biol. Inorg. Chem.* **2018,** *23* (1), 137-154.
41. Flinta, C.; Persson, B.; Jornvall, H.; Vonheijne, G., Sequence determinants of cytosolic N-terminal protein processing. *Eur. J. Biochem.* **1986,** *154* (1), 193-196.
42. Zaia, J.; Fabris, D.; Wei, D.; Karpel, R. L.; Fenselau, C., Monitoring metal ion flux in reactions of metallothionein and drug-modified metallothionein by electrospray mass spectrometry. *Protein Sci.* **1998,** *7* (11), 2398-404.
43. Blindauer, C. A.; Polfer, N. C.; Keiper, S. E.; Harrison, M. D.; Robinson, N. J.; Langridge-Smith, P. R. R.; Sadler, P. J., Inert site in a protein zinc cluster: Isotope exchange by high resolution mass spectrometry. *J. Am. Chem. Soc.* **2003,** *125* (11), 3226-3227.
44. Palacios, O.; Atrian, S.; Capdevila, M., Zn- and Cu-thioneins: A functional classification for metallothioneins? *J. Biol. Inorg. Chem.* **2011,** *16* (7), 991-1009.
45. Capdevila, M.; Bofill, R.; Palacios, O.; Atrian, S., State-of-the-art of metallothioneins at the beginning of the 21st century. *Coord. Chem. Rev.* **2012,** *256* (1-2), 46-62.
46. Ngu, T. T.; Stillman, M. J., Metalation of metallothioneins. *IUBMB Life* **2009,** *61* (4), 438-446.
47. Sutherland, D. E. K.; Stillman, M. J., The "magic numbers" of metallothionein. *Metallomics* **2011,** *3* (5), 444-463.
48. Chen, S. H.; Russell, D. H., How closely related are conformations of protein ions sampled by IM-MS to native solution structures? *J. Am. Soc. Mass Spectrom.* **2015,** *26* (9), 1433-1443.
49. Blindauer, C. A.; Razi, M. T.; Campopiano, D. J.; Sadler, P. J., Histidine ligands in bacterial metallothionein enhance cluster stability. *J. Biol. Inorg. Chem.* **2007,** *12* (3), 393-405.
50. Wishart, D. S.; Sykes, B. D.; Richards, F. M., The chemical-shift index - a fast and simple method for the assignment of protein secondary structure through NMR-spectroscopy. *Biochemistry* **1992,** *31* (6), 1647-1651.
51. Digilio, G.; Bracco, C.; Vergani, L.; Botta, M.; Osella, D.; Viarengo, A., The cadmium binding domains in the metallothionein isoform Cd-7-MT10 from *Mytilus galloprovincialis* revealed by NMR spectroscopy. *J. Biol. Inorg. Chem.* **2009,** *14* (2), 167-178.
52. Pennella, M. A.; Arunkumar, A. I.; Giedroc, D. P., Individual metal ligands play distinct functional roles in the zinc sensor *Staphylococcus aureus* CzrA. *J. Mol. Biol.* **2006,** *356* (5), 1124-1136.
53. Reyes-Caballero, H.; Guerra, A. J.; Jacobsen, F. E.; Kazmierczak, K. M.; Cowart, D.; Koppolu, U. M. K.; Scott, R. A.; Winkler, M. E.; Giedroc, D. P., The metalloregulatory zinc site in *Streptococcus pneumoniae* AdcR, a zinc-activated MarR family repressor. *J. Mol. Biol.* **2010,** *403* (2), 197-216.
54. Ma, Z.; Gabriel, S. E.; Helmann, J. D., Sequential binding and sensing of Zn(II) by *Bacillus subtilis* Zur. *Nucleic Acids Res.* **2011,** *39* (21), 9130-9138.
55. Osman, D.; Piergentili, C.; Chen, J. J.; Chakrabarti, B.; Foster, A. W.; Lurie-Luke, E.; Huggins, T. G.; Robinson, N. J., Generating a metal-responsive transcriptional regulator to test what confers metal sensing in cells. *J. Biol. Chem.* **2015,** *290* (32), 19806-19822.
56. Foster, A. W.; Pernil, R.; Patterson, C. J.; Robinson, N. J., Metal specificity of cyanobacterial nickel-responsive repressor InrS: Cells maintain zinc and copper below the detection threshold for InrS. *Mol. Microbiol.* **2014,** *92* (4), 797-812.
57. Leszczyszyn, O. I.; Evans, C. D.; Keiper, S. E.; Warren, G. Z. L.; Blindauer, C. A., Differential reactivity of individual zinc ions in clusters from bacterial metallothioneins. *Inorg. Chim. Acta* **2007,** *360* (1), 3-13.
58. Krezel, A.; Maret, W., The biological inorganic chemistry of zinc ions. *Arch. Biochem. Biophys.* **2016,** *611*, 3-19.
59. Peroza, E. A.; Al Kaabi, A.; Meyer-Klaucke, W.; Wellenreuther, G.; Freisinger, E., The two distinctive metal ion binding domains of the wheat metallothionein E_c-1. *J. Inorg. Biochem.* **2009,** *103* (3), 342-353.
60. Vašák, M.; Kägi, J. H. R.; Hill, H. A. O., Zinc(II), cadmium(II), and mercury(II) thiolate transitions in metallothionein. *Biochemistry* **1981,** *20* (10), 2852-2856.
61. Daniels, M. J.; Turner-Cavet, J. S.; Selkirk, R.; Sun, H.; Parkinson, J. A.; Sadler, P. J.; Robinson, N. J., Coordination of Zn^{2+} (and Cd^{2+}) by prokaryotic metallothionein. Involvement of His-imidazole. *J. Biol. Chem.* **1998,** *273* (36), 22957-22961.

62. Vašák, M., Metal removal and substitution in vertebrate and invertebrate metallothioneins. *Methods Enzymol.* **1991,** *205*, 452-458.
63. Gan, T.; Munoz, A.; Shaw, C. F.; Petering, D. H., Reaction of Cd-111(7)-metallothionein with EDTA - a reappraisal. *J. Biol. Chem.* **1995,** *270* (10), 5339-5345.
64. Huang, M.; Shaw, C. F.; Petering, D. H., Interprotein metal exchange between transcription factor IIIa and apo-metallothionein. *J. Inorg. Biochem.* **2004,** *98* (4), 639-648.
65. Osman, D.; Martini, M. A.; Foster, A. W.; Chen, J. J.; Scott, A. J. P.; Morton, R. J.; Steed, J. W.; Lurie-Luke, E.; Huggins, T. G.; Lawrence, A. D.; Deery, E.; Warren, M. J.; Chivers, P. T.; Robinson, N. J., Bacterial sensors define intracellular free energies for correct enzyme metalation. *Nat. Chem. Biol.* **2019,** *15* (3), 241-249.
66. Chen, X. H.; Chu, M. H.; Giedroc, D. P., MRE-binding transcription factor-1: Weak zinc-binding finger domains 5 and 6 modulate the structure, affinity, and specificity of the metal-response element complex. *Biochemistry* **1999,** *38* (39), 12915-12925.
67. Outten, C. E.; O'Halloran, T. V., Femtomolar sensitivity of metalloregulatory proteins controlling zinc homeostasis. *Science* **2001,** *292* (5526), 2488-2492.
68. Lomas, M. W.; Bates, N. R.; Johnson, R. J.; Knap, A. H.; Steinberg, D. K.; Carlson, C. A., Two decades and counting: 24-years of sustained open ocean biogeochemical measurements in the Sargasso Sea. *Deep-Sea Res. Part II-Top. Stud. Oceanogr.* **2013,** *93*, 16-32.
69. Pinter, T. B. J.; Stillman, M. J., Kinetics of zinc and cadmium exchanges between metallothionein and carbonic anhydrase. *Biochemistry* **2015,** *54* (40), 6284-6293.
70. Jacob, C.; Maret, W.; Vallee, B. L., Control of zinc transfer between thionein, metallothionein, and zinc proteins. *Proc. Natl. Acad. Sci. U. S. A.* **1998,** *95* (7), 3489-3494.
71. Heinz, U.; Kiefer, M.; Tholey, A.; Adolph, H. W., On the competition for available zinc. *J. Biol. Chem.* **2005,** *280* (5), 3197-3207.
72. Maret, W., Oxidative metal release from metallothionein via zinc thiol-disulfide interchange. *Proc. Natl. Acad. Sci. U. S. A.* **1994,** *91* (1), 237-241.
73. Pruteanu, M.; Neher, S. B.; Baker, T. A., Ligand-controlled proteolysis of the *Escherichia coli* transcriptional regulator ZntR. *J. Bacteriol.* **2007,** *189* (8), 3017-3025.
74. Peroza, E. A.; Cabral, A. D.; Wan, X. Q.; Freisinger, E., Metal ion release from metallothioneins: Proteolysis as an alternative to oxidation. *Metallomics* **2013,** *5* (9), 1204-1214.